Thermochimica Acta, 239 (1994) 181–199
Elsevier Science B.V., Amsterdam
SSDI 0040-6031(93)01654-L

Identification of the thermal processes in the binary $Cu(NO_3)_2 \cdot 3H_2O$ and $Cr(NO_3)_3 \cdot 9H_2O$ systems

L. Gubrynowicz

Institute of Inorganic Chemistry and Technology, Silesian Technical University, 6 Krzywoustego Street, 44-100 Gliwice, Poland

(Received 2 June 1993; in final form 16 November 1993)

Abstract

The thermal behaviour of binary $Cu(NO_3)_2 \cdot 3H_2O$–$Cr(NO_3)_3 \cdot 9H_2O$ mixtures in molar ratios 1:2 and 1:1 has been studied in air atmosphere in the temperature range 20–900°C. Relative thermal analysis has been used to detect the range of existence of individual intermediates in the decomposed mixtures. The intermediates have been isolated by isothermal heating of mixtures at desired temperatures and identified by IR spectrometry and X-ray diffractometry and also by standard and indirect quantitative chemical analysis. On the basis of the results obtained, a probable mechanism for the overall decomposition of the mentioned nitrates mixtures in the above temperature range is discussed.

INTRODUCTION

The so-called mixed oxide catalysts are often produced by the thermal decomposition of the nitrates of suitable metals (see, for example, ref. 2). This also applies to the mixed copper–chromium oxide catalysts (see, for example, refs. 3–10). Nevertheless in publications on these topics there exist contradictory opinions with respect to the preparation conditions of these products, the observed intermediates and the temperature range of their existence, and other details of their thermal treatment [11, 12]. Particularly different are the views about the formation of intermediate products in the course of the decomposition. This question is reexamined in the present paper. The course of decomposition was studied with the use of the previously described relative thermal analysis (RTA). The study addresses therefore the possibility of a simultaneous verification of practical use of the RTA method.

EXPERIMENTAL

Materials

All the chemicals used in the derivatographic studies and those for the chemical analysis and for preparation of the intermediate decomposition products, were of Analar grade (POCh, Gliwice, Poland).

Thermal analysis

Thermal tests were carried out on an automatic Paulik–Paulik–Erdey derivatograph, manufactured by MOM (Budapest, Hungary). The results from thermal analyses of single $Cu(NO_3)_2 \cdot 3H_2O$ (copper nitrate trihydrate (CNT)) and $Cr(NO_3)_3 \cdot 9H_2O$ (chromium nitrate nonahydrate (CNN)) samples and of CNT–CNN mixtures served for the construction and design of the relative thermal analytical (RTA) curves as has been described in an earlier paper [1].

Sample preparation

In order to prepare a given intermediate or final decomposition products, suitable samples of binary CNT–CNN mixtures of accepted composition were isothermally heated in a constant air flow in a pipe furnace at well-controlled temperatures selected according to the observed peaks on the RTA curves. The calcining was stopped when a constant sample mass was obtained. The gaseous decomposition products evolved from samples in the course of the process were absorbed in standard NaOH solution and analysed by acid–base titration. The solid residues after each heat treatment were allowed to cool in a desiccator at room temperature and then submitted to IR, X-ray diffractometry (XRD) and chemical analysis. Specific surface areas of the preparations were measured from Ar desorption data, obtained by the gas chromatographic (GC) method [13]. The samples derived from CNT–CNN mixtures of molar ratios (1:2) were designated later as series 18 and those of molar ratios (1:1) as series 18A. The indices to these numerations on the figures and in tables mean the temperature of sample preparation.

IR analysis

First of all IR absorption measurements were adopted for phase identification in all solid products. The loose samples were recorded on a UR-20 spectrometer (Carl Zeiss, Jena, Germany) in the range 4000–400 cm^{-1}, using the 1% KBr technique. For greasy materials, IR spectral examinations were made using a Specord 71 spectrophotometer (Carl Zeiss, Jena, Germany) equipped with an attenuated total reflection (ATR) attachment, described elsewhere [14], in the range 4000–650 cm^{-1} under the following conditions: germanium monocrystal plate, reflection angle $Q = 45°$, reflection frequency $N = 25°$. The obtained spectra were compared with the standard spectra from the catalogues of Nyquist and Kagel [15], Nakamoto [16], Swiętosławska [17] and from other sources, for example ref. 18.

X-ray analysis

X-ray diffraction measurements were carried out on a TUR-M-61 diffractometer (VEB Transformatoren- und Röntgenwerk, Dresden, Germany), using Cu Kα radiation with a nickel filter, lamp parameters of 35 kV and 20 mA, operation counter voltage 1300 V, rate of tape feeding 1200 mm h^{-1}. Diffractograms were interpreted by comparison with ASTM powder diffraction cards [19] or other XRD standards.

Chemical analysis

The solid products, formed during the decomposition processes, were also characterized by wet chemical analysis. The separation of phases was based on the differences in their solubility in various media, i.e. in water (CNT, CNN), in strong acids (basic nitrates and chromates, CuO) and in hot concentrated $HClO_4$ (Cr_2O_3, $CuCr_2O_4$, $Cu_2Cr_2O_4$) [20]. The simultaneous solubilization of all these phases was achieved by fusion with Na_2O_2 [21] or by leaching in hot $HClO_4$ or in an $HClO_4$–H_2SO_4 mixture [22]. The leaching in hot concentrated NaOH solution allowed the NO_3^- and CrO_4^{2-} ions to be extracted from samples which were insoluble in water.

The quantitative chemical analysis included the following determinations: electrolytic analysis of Cu^{2+} ions in acid solutions of samples from different extractions [23]; iodometric determination of the total ($Cr^{6+} + Cu^{2+}$) ions [24]; iodometric determination of the total ($Cr^{6+} + Cr^{3+}$) ions after electrolytic removal of Cu^{2+} ions and subsequent oxidation of Cr^{3+} to Cr^{6+} by H_2O_2 in alkaline solution [20]; determination of the OH^- ions using Steinhauser's [25] method and NO_3^- ions by back titration of the excess of standard H_2SO_4 solution, added to ammonia distillate, obtained after the reduction of nitrates with Devarda's alloy [24].

The phase composition of solid samples was then calculated indirectly, based on the results of the determinations cited above. The relative errors in particular analyses were of the order of 1–5%.

RESULTS

Relative thermal analysis

For the purpose of detecting existing intercomponent processes during the thermal decomposition of CNT–CNN mixtures relative thermal analysis (RTA) was introduced. The results of the thermal analysis of single components of the investigated mixture were taken from our earlier works, namely from ref. 26 with regard to CNT and ref. 27 concerning CNN. These experimental data are completed by results of thermal studies of binary CNT–CNN mixtures, published later [1], where the RTA curves have been constructed and demonstrated. From these last curves the RDTA

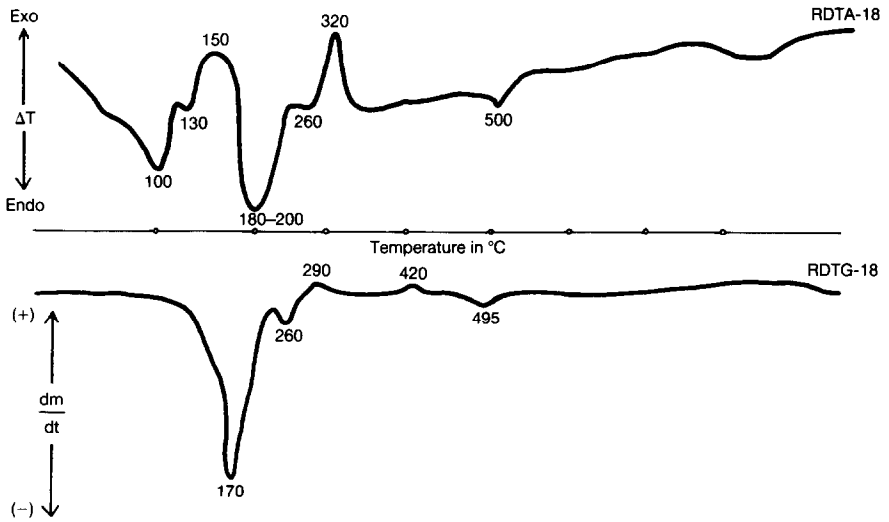

Fig. 1. Comparison of RDTA and RDTG curves for 1:2 CNT–CNN (series 18) samples.

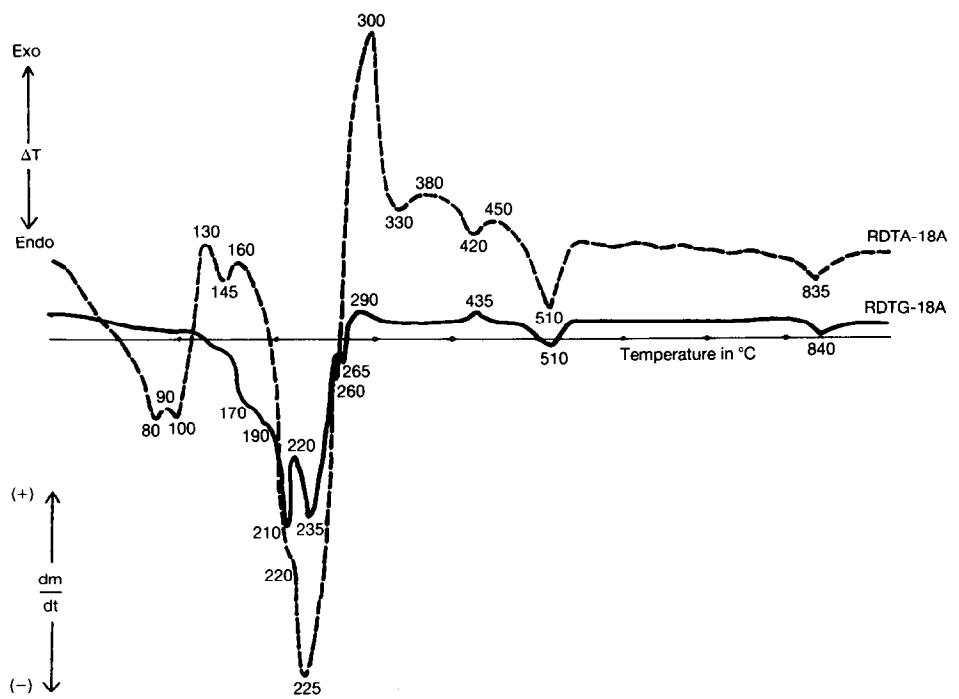

Fig. 2. Comparison of RDTA and RDTG curves for 1:1 CNT–CNN (series 18A) samples.

and RDTG curves are shown in Figs. 1 and 2 for series 18 and series 18A samples, respectively. Both series demonstrate similar additional thermal effects. Their character may be elucidated roughly by comparison of RDTA and RDTG in each series [1].

The detailed interpretation of the separate thermal effects detected on the RTA curves was performed by means of additional analytical techniques.

IR analysis

Characterization of starting materials, intermediates and end products of the thermal decomposition of CNT–CNN mixtures was performed by IR spectrometry. The observed spectra for series 18 and 18A samples calcined isothermally at different temperatures are shown in Figs. 3–5.

The initial course of the decomposition may be elucidated from spectra of the tails after distillation of molten sample at 150°C (Fig. 3). The presented spectra display various absorptions over the normal range of water vibrations (3800–1500 cm^{-1}), manifesting the existence of various types of retained water. Very broad and strong absorption peaks, one around 3400 cm^{-1} and the other around 1640 cm^{-1} confirm the presence of water in the sample [28]. Furthermore the spectrum shown contains not only absorption bands at 1050–1030 cm^{-1}, 1320 and around 1400 cm^{-1}, which exist in the IR spectra of basic chromium nitrates (BCrN) [27], but also a series of absorption bands in the 1000–700 cm^{-1} region which are assigned to chromates [15]. The presence of nitrate group in the sample causes, according to ref. 29, three normal oscillations in the spectrum at 1050 cm^{-1}, at 1310 and

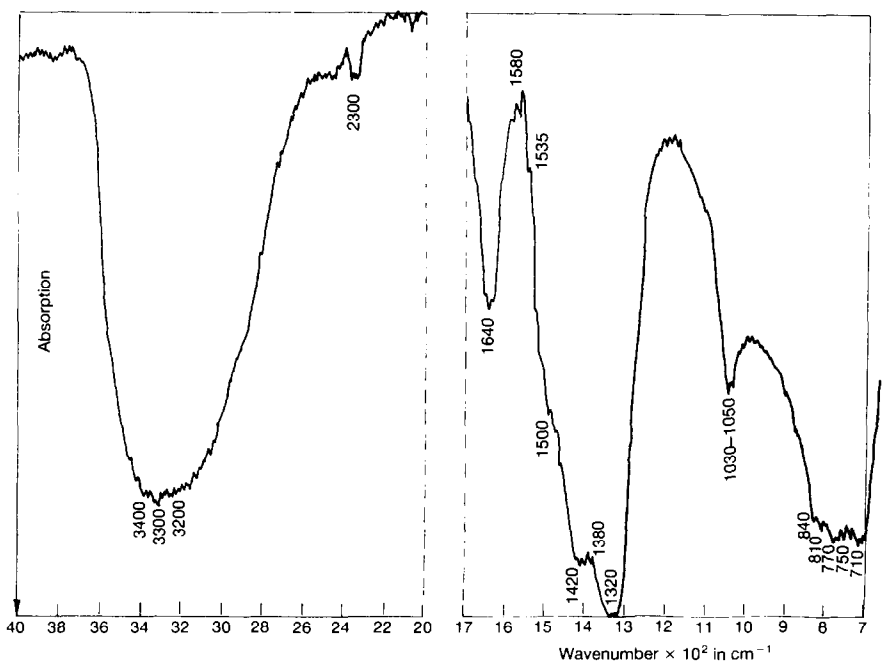

Fig. 3. IR spectrum of tails after distillation of a 1:2 CNT–CNN (series 18) sample at 150°C, obtained by the ATR technique.

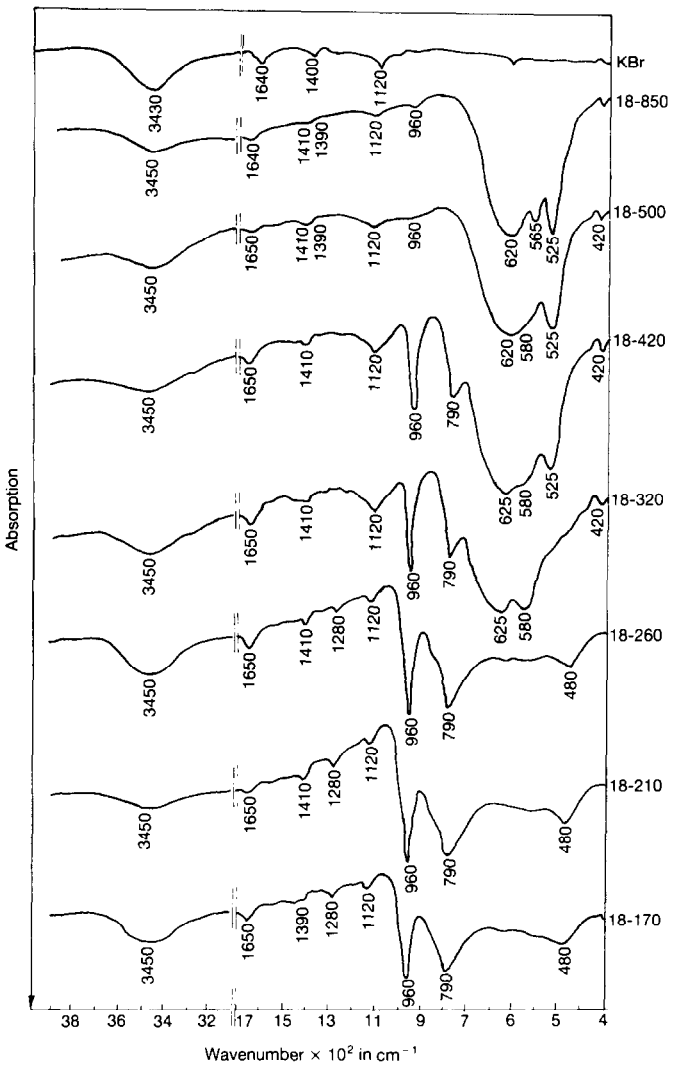

Fig. 4. IR spectra of calcination products of 1:2 CNT–CNN (series 18) samples at different temperatures, obtained by the KBr disc technique.

1410 cm^{-1}, and at 825 cm^{-1}. The presence of OH^- groups, probably attached to Cu^{2+}, can be correlated with symmetric and antisymmetric vibrations at 3428 and 3304 cm^{-1}. Some of these groups may participate in bridging bonds of the type Cu–OH–Cu or Cu–OH–Cr [30]. The bands at 1050–1030 cm^{-1} and the band at around 3400 cm^{-1} suggest the coexistence of chromium and copper nitrates and chromates in the form of basic salts [31].

IR absorption spectra of the decomposition products in CNT–CNN systems at higher temperatures are presented in Figs. 4 and 5. The determination of the particular phases in these products was based on the presence

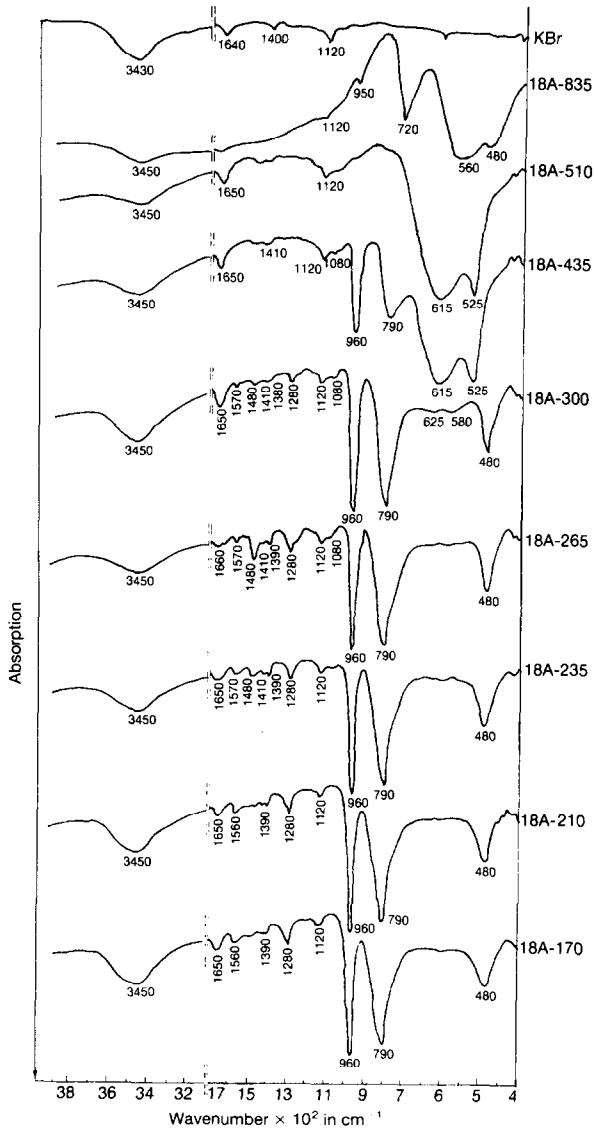

Fig. 5. IR spectra of calcination products of 1:1 CNT–CNN (series 18A) samples at different temperatures, obtained by the KBr disc technique.

of characteristic bands (cm^{-1}) in the IR spectra, at 958 s, 790 s, 479 s and 405 m for $CuCrO_4$ [18], at 645 s, 550 s, 440 m and 410 m for Cr_2O_3 [15], at 616 s, 526 s and 370 m for $CuCr_2O_4$ [18] and at 720 s, 560 s and 480 m for $Cu_2Cr_2O_4$ [15].

Contrary to expectation the spectra of chromium basic or neutral chromate (BCrC or NCrC) and of CuO were imperceptible and not detectable. Probably the spectrum of $CuCrO_4$ covers the spectra of other components. Similarly the presence of CuO was undetectable in a mixture with $Cu_2Cr_2O_4$.

All results of IR spectral analyses are shown in Table 4.

X-ray analysis

Generally the XRD analysis gave much more information than IR spectrometry, allowing nearly all constituents of the investigated mixtures to be detected. Difficulties encountered in this analysis were caused by the amorphous or poorly crystalline state of some samples, especially at lower temperatures. They were connected with the high noise level or considerable width of reflexes and therefore the overlapping of neighbouring peaks.

XRD data from the solid decomposition products of CNT–CNN mixtures obtained at different temperatures are given in Table 1 for both series of samples. Phase compositions of particular samples, deduced from com-

TABLE 1

XRD data on solid decomposition products of CNT–CNN mixtures and their acid-resistant matter (arm)

Sample	*d* spacing/Å	Phases present [a]
18-180	4.87vw, 3.66m, 3.56m, 2.72w, 2.61w, 2.49m	A, B
18-260	4.85vw, 3.65s, 3.56s, 2.72m, 2.61m, 2.49s	A, B
18-290	4.90vw, 3.66s, 3.57s, 2.72m, 2.62m, 2.49s	A, B
18-320	4.85vw, 3.64s, 3.57s, 2.72w, 2.66s, 2.61m, 2.49s, 2.31vw	A, B, C, D
18-420	4.78vw, 3.66vw, 3.57vw, 3.04vw, 2.67vw, 2.54w, 2.52m 2.49vw, 2.39w, 2.32w	A, C, D, E
18-500	4.78vw, 3.63vw, 3.04vw, 2.67vw, 2.54m, 2.53m, 2.52m 2.48vw, 2.39w, 2.32vw	C, D, E
18-850	5.69vw, 4.80vw, 3.04vw, 2.88w, 2.85m, 2.57w, 2.54s 2.47vw, 2.39s, 1.63m	F, G
18A-170	4.87w, 3.66vs, 3.56s, 2.72vs, 2.62vs, 2.49vs, 2.30vw, 1.78w	A, B, H
18A-210	4.90vw, 3.35m, 3.55m, 2.72w, 2.62w, 2.49m, 2.32w, 1.78vw	A, B, H
18A-235	4.82vw, 3.65s, 3.56s, 2.71s, 2.62s, 2.49vs, 2.30vw, 2.16w	A, B
18A-265	4.82vw, 3.65w, 3.56w, 2.71w, 2.61w, 2.49m, 2.16vw	A, B
18A-300	4.93vw, 3.68vs, 3.63vs, 3.57s, 2.72w, 2.67s, 2.62vs 2.57w, 2.49vs, 2.48vs	A, B, C
18A-330	3.66vs, 3.63s, 3.57vs, 2.75vw, 2.72s, 2.67vs, 2.62vs 2.53vs, 2.52vs, 2.49s	A, C, D
18A-435	3.66vs, 3.63s, 3.57vs, 3.04vw, 2.75w, 2.72s, 2.67w, 2.62vs 2.54m, 2.53s, 2.49vs	A, C, D, E
18A-510	4.77w, 3.01w, 2.53vs, 2.39s, 2.32s, 2.13w, 1.87w, 1.71w	D, E
18A-835	2.85vs, 2.73vw, 2.53w, 2.47vs, 2.21m, 1.90vw, 1.64m, 1.49m	D, F, G
18-320 arm	3.63w, 2.67m, 2.48m, 2.18w, 1.82vw, 1.67w	C
18-420 arm	4.78vw, 3.63vw, 3.04w, 2.67w, 2.54s, 2.48w, 2.39m, 2.18vw, 2.13w	C, E
18-500 arm	4.78vw, 3.63vw, 3.04vw, 2.67w, 2.54s, 2.48w, 2.39m, 2.18vw, 2.13w	C, E
18-850 arm	5.69vw, 4.80vw, 3.04w, 2.88m, 2.57w, 2.54s, 2.47w, 2.39s, 2.21vw	F, G
18A-330 arm	3.63w, 2.67m, 2.48m, 2.18w, 1.67w	C

Key: w, weak; m, medium; s, strong; v, very.

[a] A–H, arbitrary designations of XRD standards cited in Table 2.

TABLE 2

Reference standards used in XRD analysis of CNT–CNN mixtures

Arbitrary designation	*d* spacing/Å	PDF card [19]	Compound
A	3.66(52), 3.57(50), 2.72(45), 2.62(60), 2.49(100)	16-485	$CuCrO_4$
B	4.90(100), 3.62(45)	1-0257	$CuCrO_4 \cdot 2Cu(OH)_2$
C	3.63(75), 2.67(100), 2.48(95), 2.18(40), 1.82(40), 1.67(90)	6-504	Cr_2O_3
D	2.75(12), 2.53(49), 2.52(100), 2.32(96)	5-661	CuO
E	4.78(10), 3.04(16), 2.54(100), 2.39(60), 2.13(20)	21-874	$CuCr_2O_4$ tetrag.
F	4.80(15), 3.04(16), 2.88(50), 2.55(100), 2.39(55)	26-508	$CuCr_2O_4$ cubic
G	5.69(45), 2.85(40), 2.57(20), 2.47(100), 2.21(40)	5-668	$Cu_2Cr_2O_4$
H	2.62(80), 2.31(80), 1.78(40)	14-687	$Cu_2(OH)_3NO_3$

Relative intensities are given in parentheses.

parison of the observed d spacing values with the standard data from the powder diffraction cards [19] are completed in Table 4. The obtained XRD data were compared with XRD standards cited in Table 2.

Difficulties in verification of the presence of Cr_2O_3 in the investigated mixtures were resolved by XRD of acid-resistant matter (arm) of calcination products at different temperatures (Table 1). The obtained data show that the arm in series 18 contains Cr_2O_3 after calcination of samples at 290, 420 and 500°C as well as $CuCr_2O_4$ after thermal treatment at 420, 500 and 850°C and presumably small quantities of $Cu_2Cr_2O_4$ after heating at 850°C.

Chemical analysis of the solid products in the thermal decomposition of CNT–CNN binary systems

For more accurate examination of the composition of the particular compounds in the sinters, methods of chemical analysis were applied. The utilization of the results of IR and XRD measurements appeared, however, to be necessary for final interpretation and confirmation of phase compositions.

The chemical analysis in the present study included the determinations of the total Cu, Cu arm, Cr^{3+}, CrO_4^{2-}, NO_3^- and OH^- ion content. The results of these analyses are presented in Table 3.

On the basis of the analytical data, presented in Table 3 an indirect chemical analysis was performed, which allowed precise determinations of phase composition at all stages of thermal decomposition of CNT–CNN systems. The results of these calculations are completed in Table 4 and compared with results of other types of analysis.

DISCUSSION AND CONCLUSIONS

RTA, supplemented by IR, XRD and chemical analyses of solid decomposition products from isothermal decomposition studies in the temperature range 20–900°C, leads to the conclusion that the decomposition of $Cu(NO_3)_2 \cdot 3H_2O$–$Cr(NO_3)_3 \cdot 9H_2O$ mixtures involves the following successive physical and chemical processes during the rise of temperature.

Stage 1, 60–80°C

The CNT–CNN mixtures begin to decompose above the melting point of CNN, i.e. at around 60°C. This stage includes the endothermic melting of CNN, then an endothermic dissolution of CNT in the melt and also endothermic processes of thermal hydrolysis of both salts, occurring independently in the system according to reactions (1) [26] and (2) [27]

$$2Cu(NO_3)_2 \cdot 3H_2O = Cu_2(HO)_3NO_3 + 3HNO_3 + 3H_2O \quad (1)$$

TABLE 3

Results of chemical analysis of the decomposition products of CNT–CNN mixtures at different temperatures (series 18 and 18A)

Sample	Chemical composition/%								Molar ratios		Specific surface/ $m^2 g^{-1}$
	Cr_{tot}	Cr^{3+}	Cr^{6+}	CrO_4^{2-}	Cu_{tot}	Cu_{arm}	OH^-	NO_3^-	$\frac{Cr_{tot}}{Cu_{tot}}$	$\frac{Cr^{6+}}{Cr^{3+}}$	
18-150	33.5	20.9	12.6	28.1	20.5	–	20.6	10.0	2.0	0.6	–
18-180–200	37.3	15.5	21.8	48.5	22.8	–	13.2	–	2.0	1.4	36.6
18-260	38.1	15.9	22.2	49.6	23.3	–	9.3	–	2.0	1.4	–
18-290	39.0	10.4	28.6	63.8	23.8	–	–	–	2.0	2.8	–
18-320	42.6	28.6	14.0	31.2	25.7	–	–	–	2.0	0.5	–
18-420	43.4	36.2	7.2	16.1	26.5	13.3	–	–	2.0	0.2	5.2
18-500	44.9	44.9	0.0	0.0	27.5	27.5	–	–	2.0	0.0	4.8
18-850	44.9	44.9	0.0	0.0	27.5	27.5	–	–	2.0	0.0	1.5
18A-160	24.2	14.5	9.7	21.6	29.6	–	19.8	14.4	1.0	0.7	–
18A-170	28.4	8.9	19.4	43.4	31.1	–	11.3	5.3	1.0	2.2	–
18A-210	27.6	6.9	20.7	46.2	33.7	–	10.5	2.7	1.0	3.0	–
18A-235	28.1	7.0	21.1	47.0	34.4	–	11.5	–	1.0	3.0	–
18A-265	29.6	7.4	22.2	49.5	36.1	–	2.4	–	1.0	3.0	–
18A-300	29.5	3.9	25.6	57.1	36.0	–	–	–	1.0	6.5	18.0
18A-330	30.3	10.1	20.2	45.1	37.0	–	–	–	1.0	2.0	–
18A-435	31.8	21.2	10.6	23.6	38.9	6.5	–	–	1.0	0.5	–
18A-510	33.4	33.4	–	–	40.8	20.4	–	–	1.0	0.0	4.0
18A-840	35.2	35.2	–	–	43.1	43.1	–	–	1.0	0.0	3.0

$$2Cr(NO_3)_3 \cdot 9H_2O = CrOH(NO_3)_2 + Cr(OH)_2NO_3 + 3HNO_3 + 15H_2O \quad (2)$$

with the vaporization of HNO_3. The course of these processes as independent ones, has not been detected on the RTA curves.

Stage 2, 80–100°C

The elimination of HNO_3 leads to a gradual rise of pH in the melt and then to the precipitation or coprecipitation of intermediate basic nitrates of both metals. It is well known in the literature that the interaction of metal hydroxides or hydroxysalts during the coprecipitation is due to the formation of hydroxy bridges [32] and that the hydroxide groups appear to crosslink the cations of different metals [33] or that the intermediate products during the coprecipitation of sparingly-soluble hydroxides are polymolecular hydroxy complexes or complex salts [34], which are later transformed into so called "primary particles" [34], "parent phases" or "parent matter" [35].

According to Erenburg et al. [36] coprecipitates, obtained from the solution of copper and chromium nitrates of different ratios, probably consist of double copper and chromium hydroxynitrates or double hydroxides. Their exact composition has not been determined.

TABLE 4

Summary list of phases detected in the calcination products by means of particular analytical techniques used

Sample	IR spectrometry	X-ray diffractometry	Approximate stoichiometry after chemical analysis
18-150	Basic nitrates and chromates of Cu and Cr	Amorphous substances	$2Cr_2(OH)_4CrO_4 + CrOHCrO_4 + 2Cu_2(OH)_3NO_3$
18-180–200	$CuCrO_4$	$CuCrO_4$, $CuCrO_4 \cdot 2Cu(OH)_2$	$3CuCrO_4 + CuCrO_4 \cdot 2Cu(OH)_2 + 2Cr_2(OH)_4CrO_4 + CrOHCrO_4$
18-260	$CuCrO_4$	$CuCrO_4$, $CuCrO_4 \cdot 2CuO$	$3CuCrO_4 + CuCrO_4 \cdot 2CuO + 2Cr_2(OH)_4CrO_4 + CrOHCrO_4$
18-290	$CuCrO_4$	$CuCrO_4$, $CuCrO_4 \cdot 2CuO$	$15CuCrO_4 + 5CuCrO_4 \cdot 2CuO + 8Cr_2(CrO_4)_3$
18-320	$CuCrO_4$, Cr_2O_3	$CuCrO_4$, $CuCrO_4 \cdot 2CuO$, Cr_2O_3, CuO	$7CuCrO_4 + CuCrO_4 \cdot 2CuO + 2CuO + 8Cr_2O_3$
18-320 arm	Cr_2O_3		
18-420	$CuCrO_4$, Cr_2O_3, $CuCr_2O_4$	$CuCrO_4$, $CuCr_2O_4$ tetrag., Cr_2O_3, CuO	$2CuCrO_4 + 3CrCr_2O_4 + CuO + 2Cr_2O_3$
18-420 arm		$CuCr_2O_4$ tetrag., Cr_2O_3	
18-500	Cr_2O_3, $CuCr_2O_4$	$CuCr_2O_4$ tetrag., Cr_2O_3, CuO	$CuCr_2O_4$
18-500 arm		$CuCr_2O_4$ tetrag., Cr_2O_3	
18-850	$CuCr_2O_4$, Cr_2O_3, $(Cu_2Cr_2O_4)$	$CuCr_2O_4$ cubic, $Cu_2Cr_2O_4$	$CuCr_2O_4$
18-850 arm		$CuCr_2O_4$ cubic, $Cu_2Cr_2O_4$	
18A-160		$2Cr_2(OH)_4CrO_4 + 2CrOHCrO_4 + 5Cu_2(OH)_3NO_3$	
18A-170	$CuCrO_4$	$CuCrO_4$, $CuCrO_4 \cdot 2Cu(OH)_2$, $Cu_2(OH)_3NO_3$	$CuCrO_4 + CuCrO_4 \cdot 2Cu(OH)_2 + 2CrOHCrO_4 + Cu_2(OH)_3NO_3$
18A-210	$CuCrO_4$	$CuCrO_4$, $CuCrO_4 \cdot 2Cu(OH)_2$, $Cu_2(OH)_3NO_3$	$CuCrO_4 + CuCrO_4 \cdot 2Cu(OH)_2 + 2CrOHCrO_4 + Cu_2(OH)_3NO_3$
18A-235	$CuCrO_4$	$CuCrO_4$, $CuCrO_4 \cdot 2Cu(OH)_2$	$CuCrO_4 + CuCrO_4 \cdot 2Cu(OH)_2 + CrOHCrO_4$
18A-265	$CuCrO_4$	$CuCrO_4$, $CuCrO_2 \cdot 2CuO$	$CuCrO_4 + CuCrO_4 \cdot 2CuO + CrOHCrO_4$
18A-300	$CuCrO_4$, Cr_2O_3	$CuCrO_4$, $CuCrO_4 \cdot 2CuO$, Cr_2O_3	$15CuCrO_4 + 5CuCrO_4 \cdot 2CuO + 2Cr_2(CrO_4)_3$
18A-330		$CuCrO_4$, CuO, Cr_2O_3	$20CuCrO_4 + 10CuO + 5Cr_2O_3$
18A-330 arm		Cr_2O_3	
18A-435	$CuCrO_4$, $CuCr_2O_4$	$CuCrO_4$, CuO, Cr_2O_3, $CuCr_2O_4$ tetrag.	$2CuCrO_4 + 3CuO + Cr_2O_3 + CuCr_2O_4$
18A-510	$Cu_2Cr_2O_4$	CuO, $CuCr_2O_4$ tetrag.	$CuO + CuCr_2O_4$
18A-835	$Cu_2Cr_2O_4$	$Cu_2Cr_2O_4$ (traces of $CuO + CuCr_2O_4$)	$Cu_2Cr_2O_4$

Below 100°C no or insignificant changes of mass were observed in the RDTG curves, while in the RDTA curves distinct endothermic effects at 100°C (series 18) and at 80 and 100°C (series 18A) are strongly marked, which are presumably connected with the melting of the above mentioned "parent matter".

Stage 3, 100–150°C

The decomposition of the examined mixtures during this stage is of exothermic character. Above 100°C a distinct distillation of HNO_3 is observed, resulting in the shift of the hydrolysis equilibrium of chromium salts to the right and formation of compounds with a higher degree of basicity

$$CrOH(NO_3)_2 + H_2O = Cr(OH)_2NO_3 + HNO_3 \quad (3)$$

The boiling of the melt with the azeotropic mixture HNO_3–H_2O, observed at 120–130°C, can also result in partial oxidation of Cr(III) compounds (evidenced by the liberation of NO_2 or NO) according to

$$3Cr(OH)_2^+ + 2NO_3^- = CrOHCr_2O_7 + 2NO + 2H_2O + H^+ \quad (4)$$

$$2Cr(OH)_2^+ + NO_3^- = CrOHCrO_4 + NO + H_2O + H^+ \quad (5)$$

and the formation of basic chromium dichromates and chromates [27]. The small endothermic effects at 130°C (series 18) and 145°C (series 18A) may be connected with the thermal decomposition of the above cited "parent matter" and elimination of HNO_3 together with its reduction products. The total exothermic character of this stage is probably due to the domination of the heat of oxidation of Cr(III) compounds over the heat of decomposition of NO_3^- ions and "parent matter". During the evaporation of the melt the precipitation of basic copper chromate (BCuC) is also possible [37, 38]

$$Cu_2(OH)_3^+ + CrO_4^{2-} + OH^- = CuCrO_4 \cdot 2Cu(OH)_2 \quad (6)$$

This stage comes to an end with the complete evaporation of liquid from the melt at about 150°C.

Stage 4, 150–235°C

Between 150 and 170°C the strong mass loss on the RDTG-18 curve starts, associated with the endothermic peak on the RDTA-18 curve with a minimum at 180–200°C, as a result of the emission of HNO_3 and NO_2 and nearly complete denitrification of the residue. The chemical processes, taking place in this range may be represented by eqns. (3) and (5) and then (7) and (8) [27].

$$3Cr(OH)_2NO_3 = Cr_2(OH)_4CrO_4 + 3NO + H_2O \quad (7)$$

$$Cr(OH)Cr_2O_7 + Cr(OH)_2NO_3 = 2CrOHCrO_4 + HNO_3 \quad (8)$$

Since BCuN alone is thermally persistent to above 190°C [26], it is evident that this compound reacts earlier with accompanied BCrC and forms BCuC according to

$$3Cu_2(OH)_3NO_3 + Cr_2(OH)_4CrO_4 + CrOHCrO_4 = 2CuCrO_4 \cdot 2Cu(OH)_2 + 3Cr(OH)_2NO_3 \quad (9)$$

Basic copper chromates [9, 37–41], represent a very broad group of chromates with various values of the $CuCrO_4/Cu(OH)_2$ ratio [41]. They can be precipitated from solution over a wide range of Cu^{2+} and CrO_4^{2-} concentrations in the form of hydrates [38]. They are formed according to reaction (9) and are thermally stable up to 260–265°C [39, 40], whereas the $Cr(OH)_2NO_3$ simultaneously formed in these conditions is immediately converted into $Cr_2(OH)_4CrO_4$ via reaction (7) as was proved earlier [27].

The above cited conversions are mainly of endothermic character and are associated with mass losses on RTA curves in series 18. Similar behaviour was also observed in series 18A. Here, however, two negative RDTA effects at 210 and 235°C are observed, corresponding to a common peak on the RDTG curve at 225°C. This disagreement in the thermal behaviour between the series is difficult to explain at the moment.

Furthermore, in this stage at 170, 210 and 235°C the existence of neutral copper chromate (NCuC) is detected. This suggests the possibility of a parallel side reaction

$$Cu_2(OH)_3 + CrOHCrO_4 = 2CuCrO_4 + NO + 2H_2O \quad (10)$$

between the intermediates BCrC and BCuC, which proceeds at a temperature no lower than 170°C.

Stage 5, 260–265°C

The next stage of the thermal decomposition takes place from 260 to 265°C and is connected with the distinct negative peaks on both RTA curves. These effects are unequivocally related to the dehydration process of BCuC to anhydrous basic copper chromate (BCuCA), already described in the literature [39, 40], which occurs at exactly these temperatures according to

$$CuCrO_4 \cdot Cu(OH)_2 = CuCrO_4 \cdot 2CuO \cdot 2H_2O = CuCrO_4 \cdot 2CuO + 2H_2O \quad (11)$$

It must be strongly emphasized that other basic copper chromates are submitted to the dehydration process at other temperatures [41] and this confirms the presence of $CuCrO_4 \cdot 2Cu(OH)_2$ in the system.

Stage 6, 290–320°C

This stage includes the strong positive peaks on both RTA curves with maxima at 290–320°C (series 18) and 290–300°C (series 18A), and is connected with the increase of Cr^{6+} concentration (see Table 3). The increase of Cr^{6+} content above 235°C proceeds in the absence of NO_3^- ions in the system and must be generated only by oxygen in the atmosphere reacting with Cr^{3+} ions creating additional quantities of NCrC and NCuC. BCrC undergoes oxidation to NCrC according to

$$20CrOHCrO_4 + 3O_2 = 8Cr_2(CrO_4)_3 + 10H_2O \quad (12)$$

which later reacts with BCuCA to give NCuC

$$2Cr_2(CrO_4)_3 + 5CuCrO_4 \cdot 2CuO + 3O_2 = 15CuCrO_4 \quad (13)$$

The maximum content of chromates after heating at 290–320°C appears, however, to be lower than the values calculated for the complete oxidation of BCrC to NCuC (in series 18A) or to (NCuC + NCrC) mixture (in series 18). Apparently in practice reaction (13) does occur under these conditions and a part of copper stays in the system as BCuCA. Finally, in this stage small quantities of hydrated forms of Cr_2O_3 are recorded, probably as the result of the initiated decomposition process of NCrC to Cr_2O_3 according to the scheme

$$2Cr_2(CrO_4)_3 = 5Cr_2O_3 + 4.5O_2 \quad (14)$$

$$Cr_2(CrO_4)_3 \rightarrow Cr_2O_3 \cdot 2CrO_3 \rightarrow Cr_2O_3 \cdot CrO_3 \rightarrow Cr_2O_3 \quad (15)$$

Stage 7, 320–450°C

In this stage of thermal decomposition the course of the process in both series is quite different. In series 18 both RTA curves are nearly horizontal, indicating the absence of any reaction. It is however well known [27] that in these conditions the independent decomposition of NCrC to Cr_2O_3 may occur, which at 420°C causes the so called "glow phenomenon" [42], connected also with oxygen incorporation. Therefore on the RTA-18 curves a positive effect is present at about 420°C.

In series 18A the course of decomposition is apparently irregular and very difficult to explain because of the overlapping of several constituent processes.

First of all in this stage a violent decomposition of NCrC proceeds [43, 44] according to eqn. (14), as described earlier.

A possible second parallel thermal process, namely the slow and gradual formation of NCuC from BCuCA is also observed, leading to the separation of free CuO according to

$$CrO_4 \cdot 2CuO = CuCrO_4 + 2CuO \quad (16)$$

Such a conversion has already been described in the literature for different temperatures in range 350–450°C, e.g. [41, 45]. We think that reaction (16) is complete at 330°C, where the minimum on the RDTA-18A curve without change of mass is marked, but the presence of BCuCA cannot be confirmed by analysis. NCuC formed in the process is stable up to about 450°C and is probably responsible for the positive thermal effect at 380°C on the RDTA curve without change on the RDTG curve (presumably an effect of crystallization of NCuC or CuO).

The third thermal process initiated in this region is presented by the exothermic conversion of freshly formed CuO and Cr_2O_3 to $CuCr_2O_4$ spinel, which was detected by all types of analysis. Such a synthesis

$$CuO + Cr_2O_3 = CuCr_2O_4 \quad (17)$$

has often been mentioned earlier [9, 46] as proceeding at about 450°C [10, 45, 47]. This conversion is of exothermic character and causes the positive peak on the RDTA-18A curve at 450°C at the end of the stage. The effect of a "glow phenomenon" in this series and the increase of mass are marked only on the RDTG-18A curve at 435°C as a positive peak.

Stage 8, 495–510°C

This stage includes the endothermic peaks at 500°C (series 18) and 510°C (series 18A), associated with the negative effects on RDTG curves. From the analytical results on samples obtained under these conditions the decay of NCuC and further formation of $CuCr_2O_4$ is evident, while some free CuO and Cr_2O_3 were also detected in series 18. The thermal decomposition of NCuC may be ascribed to two different chemical processes, but most often to the conversion which gives directly an equimolecular mixture of $CuCr_2O_4 + CuO$ according to

$$2CuCrO_4 = CuCr_2O_4 + CuO + 1.5O_2 \quad (18)$$

often cited in the literature, e.g. [3, 10, 12]. The conversion proceeds over a broad range of temperature, mainly between 450 and 525°C. For the second method of thermal decomposition of NCuC the two-stage conversion is considered: first to the mixture of oxides with the elimination of O_2

$$2CuCrO_4 = 2CuO + Cr_2O_3 + 1.5O_2 \quad (19)$$

and the subsequent synthesis of spinel from oxides according to eqn. (17). These reactions proceed in the temperature range 465–505°C [18, 41, 45, 46].

Taking into account the fact that Cr_2O_3 was detected by IR spectrometry during the decomposition of NCuC, whilst XRD showed a mixture of Cr_2O_3 and CuO, then $CuCr_2O_4$ must be formed mainly by the solid-state reaction between the Cu(II) and Cr(III) oxide, according to eqn. (17). Some

workers, e.g. [9, 46], accept that the presence of $CuCr_2O_4$ in the system accelerates the direct creation of spinel from NCuC without the foregoing formation of oxides (autocatalytic effect).

Thermal decomposition of NCuC appears to be complete at about 500–510°C, when the loss of mass stops.

Stage 9, 560–800°C

In this temperature range the broad hump on the RDTA-18 curve is observed without the corresponding changes on the RDTG curve. This phenomenon may be explained as an exothermic effect of the polymorphic transformation of the tetragonal $CuCr_2O_4$ formed at 420–500°C into the cubic crystal structure, according to

$$CuCr_2O_4(\text{tetrag.}) \rightleftarrows CuCr_2O_4(\text{cubic}) \quad (20)$$

as mentioned in the literature [48, 49]. This conversion is reversible and of exothermic character. This effect has not been seen in series 18A, where the other thermal conversion takes place simultaneously.

Stage 10, 835–840°C

The subsequent thermal behaviour of sample 18A is quite different as it consists of an equimolecular mixture of $CuCr_2O_4$ and CuO. In this case at 835°C a distinct endothermal effect on RDTA is noted, associated with a negative peak on the RDTG curve. Analytical data for this sample suggest the slow combination of both constituents to give $Cu_2Cr_2O_4$ with the liberation of O_2 according to

$$CuCr_2O_4 + CuO = Cu_2Cr_2O_4 + 0.5O_2 \quad (21)$$

which causes the observed mass loss. This reaction comes readily to an end below 900°C. Some authors have published different or similar values of the temperature for this conversion between 800 and 900°C, e.g. [30, 41]. The above data rather confirm the results from our study. All the analytical methods used detected unequivocally the presence of $Cu_2Cr_2O_4$ as the principal component in the residue after calcination.

ACKNOWLEDGEMENTS

The author thanks Dr T. Strömich of the Silesian Technical University, Gliwice, for valuable assistance with experimental work.

REFERENCES

1 L. Gubrynowicz, A graphical method for detection of the occurrence of thermal processes in mixed systems by means of derivatography, Thermochim. Acta, 239 (1994) 201.

2 J. Malinsky, Erdöl Kohle, 24 (1971) 82.
3 R. Connor, K. Folkers and H. Adkins, J. Am. Chem. Soc., 54 (1932) 1138.
4 R.J. Farrauto and B. Wedding, J. Catal., 33 (1974) 249.
5 Yu. Ismailov, M.Yu. Sultanov and M.S. Belenkii, Izv. Vyssh. Uchebn. Zaved., Gaz, 13 (1970) 67.
6 G. Rienecker, Z. Anorg. Chem., 258 (1949) 280.
7 J.F. Roth and R.C. Doerr, Ind. Eng. Chem., 53 (1961) 293.
8 R. Schenck and F. Kurzen, Z. Anorg. Allg. Chem., 235 (1937) 97.
9 J. Schulz, I. Ebert and J. Scheve, Z. Anorg. Allg. Chem., 346 (1966) 66.
10 A.M. Sirina, A.I. Purtov, I.I. Kalinichenko and N.E. Koniukhova, Zh. Neorg. Khim., 16 (1971) 1601.
11 V. Pechanec, Collect. Czech. Chem. Commun., 41 (1976) 3267.
12 R.D. Shoup, K.E. Hoekstra and R.J. Farrauto, Am. Ceram. Soc. Bull., 54 (1975) 565.
13 N.E. Buyanova and A.P. Karnaukhov, Opredeleniye udelnoi poverkhnosti khromatograficheskim metodom iz teplovoi desorbcii Ar, Nauka, Novosibirsk, 1965.
14 M.M. Kiełkowska, M. Łapkowski and J. Strojek, Pol. Patent 206,561 (1978).
15 R.A. Nyquist and R.O. Kagel, IR Spectra of Inorganic Compounds, Academic Press, New York, 1971.
16 K. Nakamoto, IR Spectra of Inorganic and Coordination Compounds, Mir, Moscow, 1966 (in Russian).
17 J. Swiętosławska, in Physico-Chemical Handbook, WNT, Warsaw, 2nd edn., 1974, Chap. 4, p. E157 (in Polish).
18 J. Arsene, M. Lenglet, A. Erb and P. Granger, Rev. Chim. Miner., 15 (1978) 318.
19 Am. Soc. for Testing Materials (ASTM), Powder Diffraction File, Philadelphia, USA, continuous edition.
20 W. Fresenius and G. Jander, Handbuch der Analytische Chemie, Teil III, Quantitative Analyse, Band VIa, Springer Verlag, Berlin, 1958.
21 W.F. Hillebrand, in Yu. Lurye, Applied Inorganic Analysis, 2nd edn. 1953, Moscow, 1960, p. 538 (in Russian).
22 G.F. Smith, Ind. Eng. Chem., Anal. Ed., 6 (1934) 229.
23 St. Czubek (Ed.), Analytical Control in Chemical Industry, Vol. IV. Analysis of Inorganic Products, PWT, Warsaw, 1956, p. 196 (in Polish).
24 J. Minczewski and Z. Marczenko, Analytical Chemistry, Vol. 2. Quantitative Analysis, PWN, Warsaw, 1978, pp. 288, 292, 374 (in Polish).
25 O. Steinhauser, Fresenius' Z. Anal. Chem., 190 (1962) 148.
26 L. Gubrynowicz and T. Strömich, unpublished results, 1988.
27 L. Gubrynowicz and T. Strömich, Thermochim. Acta, 115 (1987) 137.
28 J. Fujita, K. Nakamoto and M. Kobayashi, J. Am. Chem. Soc., 78 (1956) 3963.
29 M. Maneva, N. Petroff and M. Pankova, J. Therm. Anal., 36 (1990) 577.
30 F. Hanic, J. Horvath and G. Plesch, Thermochim. Acta, 145 (1989) 19.
31 I.I. Kalinichenko, M. Sirina and A.I. Purtov, Zh. Neorg. Khim., 19 (1974) 1547.
32 V.I. Plotnikov and I.I. Safonov, Dokl. Akad. Nauk SSSR, 244 (1979) 1174.
33 A.O. Antropova, A.I. Purtov, I.I. Kalinichenko, Chem. Abstr., 97 (1982) 151536.
34 O.P. Krivoruchko, R.A. Buyanov and B.P. Zolotovskii, Izv. Sib. Otd. Akad. Nauk SSSR, Ser. Khim. Nauk, (2) (1980) 26.
35 T.M. Yurieva, React. Kinet. Catal. Lett., 29 (1985) 49.
36 B.G. Erenburg, V.P. Fateeva, A.I. Minkov, L.M. Shadrina and E.S. Stoyanov, Izv. Sib. Otd. Akad. Nauk SSSR, Ser. Khim. Nauk, (2) (1981) 54.
37 L.H. Kalbus and R.H. Petrucci, J. Chem. Educ., 46 (1969) 776.
38 E. Hayek, Z. Anorg. Allg. Chem., 216 (1934) 315; Chem. Abstr., 41 (1947) 6832f.
39 ASTM Powder Diffraction File, Card 1-0257.
40 Physico-Chemical Handbook, WNT, Warsaw, 1974, p. C212 (in Polish).

41 L. Walter-Levy and M. Goreaud, Bull. Soc. Chim. Fr., (3) (1973) 830.
42 S.K. Bhattacharyya, V.S. Ramachadran and J.C. Ghosh, Adv. Catal., 9 (1957) 114.
43 V.I. Gashin, B.S. Teleminskii and P.M. Lyan, Khim. Sb., (1972) 58; C.A. 82 (1975) 92459.
44 I.H. Park, Bull. Chem. Soc. Jpn., 45 (1972) 2749.
45 M.S. Kosnyreva, A.I. Purtov, I.I. Kalinichenko and N.M. Dorofeeva, Zh. Prikl. Khim., 49 (1976) 2515.
46 H. Charcosset, P. Turlier and Y. Trambouze, J. Chim. Phys. Chim. Biol., 61 (1964) 1249.
47 G. Kainz and H. Horvatisch, Z. Anal. Chem., 177 (1960) 344.
48 L.A. Reznitskii, Izv. Akad. Nauk SSSR, Neorg. Mater., 9 (1973) 435.
49 V.M. Ustyantsev and V.P. Marevich, Izv. Akad. Nauk SSSR, Neorg. Mater., 9 (1973) 336.